Titre: Title:	Mode-selective photonic lanterns with double-clad fibers
Auteurs: Authors:	Rodrigo Itzamna Becerra Deana, Martin Poinsinet De Sivry-Houle, Stéphane Virally, Caroline Boudoux, & Nicolas Godbout
Date:	2025
Type:	Article de revue / Article
Référence: Citation:	Becerra Deana, R. I., Poinsinet De Sivry-Houle, M., Virally, S., Boudoux, C., & Godbout, N. (2025). Mode-selective photonic lanterns with double-clad fibers. Journal of Lightwave Technology, 43(12), 5829-5835. https://doi.org/10.1109/jlt.2025.3555793

URL de PolyPublie: PolyPublie URL:	https://publications.polymtl.ca/64406/
Version:	Version officielle de l'éditeur / Published version Révisé par les pairs / Refereed
Conditions d'utilisation: Terms of Use:	Creative Commons Attribution 4.0 International (CC BY)

Document publié chez l'éditeur officiel
Document issued by the official publisher

Titre de la revue: Journal Title:	Journal of Lightwave Technology (vol. 43, no. 12)
Maison d'édition: Publisher:	IEEE
URL officiel: Official URL:	https://doi.org/10.1109/jlt.2025.3555793
Mention légale: Legal notice:	This work is licensed under a Creative Commons Attribution 4.0 License. For more information, see https://creativecommons.org/licenses/by/4.0/

Mode-Selective Photonic Lanterns With Double-Clad Fibers

Rodrigo Itzamná Becerra-Deana ⓘ, Martin Poinsinet de Sivry-Houle, Stéphane Virally ⓘ, *Member, IEEE*, Caroline Boudoux, and Nicolas Godbout ⓘ

Abstract—We present the design, fabrication, and characterization of mode-selective photonic lanterns using double-clad fibers. Here, we exploited several custom-pulled double-clad fibers to achieve the symmetry break required to excite higher-order modes. The resulting components are short and exhibit high modal isolation and low excess loss. They address some of the limitations of existing photonic lanterns in terms of fragility and coupling efficiency. The fabrication process involves the use of lower-index capillary tubes to maintain fiber geometry during fusion and tapering. Through the use of varying first cladding diameters, mode selectivity is achieved without sacrificing single-mode compatibility. This in turn allows proper real-time characterization during the whole fabrication process. Results demonstrate that double-clad fibers stacked inside a fluorine-doped capillary tube feature high modal isolation (above 60 dB) and low excess loss (lower than 0.49 dB), over a broad wavelength range (more than 250 nm) with steeper taper profiles, and more robust components. The use of less expensive synthetic fused silica capillary tubes achieves high modal isolation (above 20 dB) and excess loss lower than 2 dB over the same broad wavelength range.

Index Terms—Double-clad optical fibers, mode selectivity, optical fiber components, photonic lanterns.

I. INTRODUCTION

FIBER-BASED space-division multiplexers, also known as photonic lanterns (PLs), were introduced in 2005 as reversible multimode to single-mode multiplexers [1]. These fiber-based devices are designed for streamlined integration into compact, alignment-free optical systems. Three main types of spatial-mode multiplexers/demultiplexers are fully compatible with light injection into and collection from fibers [2]. The Multi-Plane Light Conversion (MPLC) technique generates multiple transverse modes using phase plane masks. MPLCs are capable of generating up to 1035 modes, and their dimensions are relatively modest (around 100 mm³ to 10 cm³). Their main drawback is higher excess losses (over 3 dB) [3], [4], [5], [6], [7], [8]. Additionally, mode-selective couplers can be fabricated using the polished coupler technique [9], [10], with minimal losses around 0.2 dB [11]. One of their limitations is their inability to couple to more than one higher-order mode per device. Several modes can be coupled together, but only in a cascaded configuration, which increases the total length of the system [12]. The final type of transverse mode multiplexer-demultiplexer is the mode-selective photonic lanterns (MSPLs), which is the main topic of this paper. In a modest size package of a few centimeters, it offers an efficient conversion and is a potentially lossless device with proper fabrication [13]. Its main drawback so far is the limited number of transverse modes that can be multiplexed, with a reported maximum of 15 modes so far [14]. MSPLs are widely used across multiple disciplines, including astrophysics, telecommunications, and biophotonics, and for many applications such as illumination, spectroscopy, imaging, and efficient scattering collection [15], [16], [17], [18], [19], [20], [21], [22]. They are usually fabricated by fusing and tapering several ($N \geq 2$) fibers to generate a few-mode or multimode guiding structure with a few tens of micrometers diameter. The plurality of design possibilities gives rise to distinct types of PLs. Among them, MSPLs act as mode sorters, allowing the guided transverse modes of the multimode section to be selectively coupled to a specific single-mode fiber [23]. MSPLs usually feature high modal isolation, and their operation is broadband, up to a bandwidth of 500 nm [2], with excess loss usually lower than 1 dB [13].

Some applications of PLs, such as biomedical imaging and sensing, require sturdy devices capable of being embedded in portable packages. This, in turn, implies the design of shorter components, as long fiber components tend to be much more fragile. The limiting factor in such designs is the adiabatic criterion [24]: a number characterizing the steepest slope at any taper point that allows an adiabatic transfer of modes. A higher adiabatic criterion allows steeper slopes, leading to shorter components. Previous attempts at reducing the length of PLs have included designs at the limit of existing adiabatic criterion graphs with regular single-mode fibers [25]. Unfortunately, this technique is limited by current single-mode fiber technology. Another way is to use graded-index fibers [26] with logarithmic refractive index distributions [27]. This has proven effective in increasing the adiabatic criterion and thus reducing the size of the devices.
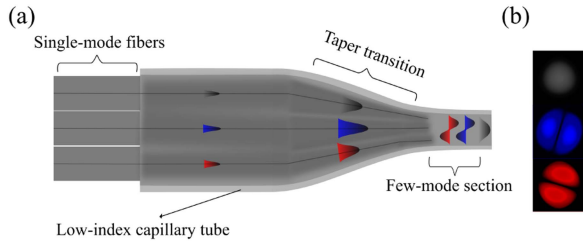
Fig. 1. Schematic of a 3×1 photonic lantern. (a) From left to right: three single-mode fibers are inserted into a low refractive index capillary tube before being fused and tapered down towards the few-mode section. Image not to scale: the outer diameter of the single-mode fibers is 125 μm, while the outer diameter of the few-mode structure is approximately 10 μm. (b) Optical profile of the three output modes akin to LP_{10} (black), LP_{11a} (blue), and LP_{11b} (red).

Single-mode compatibility (the ability of a fiber to be spliced to a single-mode fiber without any loss due to mode-mismatch) is required for lossless components. Graded-index fibers used to increase adiabatic criteria are multi-mode and thus always generate mode-mismatch losses when spliced to single-mode fibers [28], [29], [30], [31]. The same thing actually also occurs with double-clad fibers (DCFs) for which the core diameter is changed. In contrast, changes in the outer diameter of the first cladding can be made without losing single-mode compatibility. This allows for lossless splices and accurate in-situ monitoring of all loss mechanisms, as explained below.

In this paper, we demonstrate the use of DCFs with single-mode cores to design and fabricate MSPLs with increased adiabatic criteria and excellent compatibility with single-mode fibers. The components fabricated using this technique prove to be short and sturdy. They also feature high modal isolation and low excess loss.

II. DESIGN AND FABRICATION

MSPLs are composed of three main sections: a single-mode fiber bundle, a tapered transition, and a few- or multimode structure. Fig. 1 presents the longitudinal view of a 3×1 MSPL encased inside a fluorine-doped capillary tube to constrain the fiber geometry during the fusion and tapering process.

A. Design

The design of PLs involves a large number of degrees of freedom, including the number of fibers, their types, the stacking configuration, the degree of initial fusion, and the tapering profile [2], [32], [33], [34]. In an MSPL, each fiber in the single-mode bundle must exhibit a distinct refractive index profile to break the symmetry and allow to selectively excite individual transverse modes within the few-mode structure. Given the size of the design parameter space, we use SuPyMode [24], a Python-based simulation tool that uses coupled-mode theory to efficiently compute the adiabatic criterion given the characteristics of the input fiber bundle and the initial degree of fusion. SuPyMode allows rapid iteration and convergence towards adequate fiber parameters for most applications.

DCFs can be designed to offer full compatibility with single-mode fibers. They offer an important advantage over single-mode fibers used in some applications: when DCFs are tapered,

the lower-order modes remain contained inside the first cladding even as the core ceases to guide them. In applications such as PLs, this containment mechanism helps to increase the adiabatic criterion [11], [24], [35], [36], albeit to a lesser degree than with graded-index fibers. Containment in DCFs can be achieved with a large variety of first-cladding diameters without changing the diameter of the core. This greatly increases the versatility of designs, while preserving full compatibility with single-mode fibers, a feature difficult to replicate with graded-index fibers. In contrast to [36], we vary the outer diameter of the first cladding, not the diameter of the core. This enables the devices reported herein to be fully compatible with (i.e., spliced without loss to) single-mode fibers and to monitor in-situ and accurately report all excess losses.

B. Fabrication

Low-index capillary tubes are used during the fabrication process to constrain the fibers' geometry and provide additional containment in the tapered section. A capillary tube is first tapered in its center using an automated glass processing system (GPX-3000 Vytran, Thorlabs, NJ, USA) with an FTAT4 filament (Thorlabs, NJ, USA). In a 3×1 MSPL, the tube is tapered down to an inner diameter of 270 μm to constrain the three-fiber bundle into an equilateral triangle configuration over a length of 20 mm to provide adequate scanning length. Once the proper fiber configuration is obtained, a fusion step is performed, which slightly decreases the bundle size. The tapering process further reduces the few-mode or multimode part of the PL to its final size, around 10 to 20 μm. The single-mode compatibility of the DCFs fibers with SMF28 allows monitoring the fabrication process in real-time by injecting light into any input and measuring the power at all outputs.

Fig. 2 shows the in-situ characterization process of a 3×1 MSPL, with inputs connected through an in-house built optical switch to a broadband laser (BBS1550, JDS Uniphase, AZ, USA), centered at 1550 nm with a bandwidth of 50 nm. The component is placed on a heat-and-pull fabrication station, which consists of two holders with homemade clamps mounted on translation stages symmetrically arranged around a moving torch. Outputs are connected to an optical switch (built in-house) to monitor output sequentially on an optical spectrum analyzer (OSA, model AQ6317, Ando, Japan). This setup allows modal isolation and excess loss to be monitored in real-time after establishing a baseline. Any loss due to micro-deformations, dust, and unwanted coupling between modes can be observed in real-time, and the recipe can be altered accordingly, or the process can be halted immediately. We fabricate the devices in a symmetrical manner to produce two lanterns simultaneously. As a result, the losses reported in the figures are, in fact, double the losses expected for a single device, as they comprise both tapered regions.

III. RESULTS

Here, we describe the design, fabrication, and characterization of 3×1 MSPLs using DCFs. Three distinct DCFs were custom-designed (2058I1, 2058K1, and 2058J1, Université Laval, Prof. Messaddeq, QC, CA) to offer single-mode operation at 1550 nm,
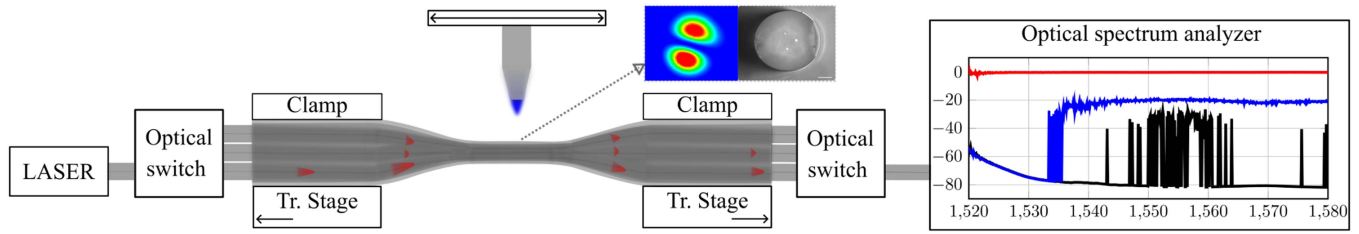
Fig. 2. Schematic diagram of the fusion tapering station, comprising a flame, clamps, and translation stages, attached to a full *in situ* characterization system comprising a laser, optical switches, and an optical spectrum analyzer. Optical switches allow for all inputs to be illuminated and all outputs to be monitored independently. Inset: one of the LP_{11} modes (left) and image of the few-mode section, both observed post cleave.

matching the mode-field diameter of telecommunication SMF-28 (ITU-T G.657.A1, Corning, NY, USA) fibers. The fibers featured three different first cladding diameters (19.6, 26.8, and 42 μm, respectively) without noticeable differences in their single-mode operation and with a numerical aperture of 0.13 between the core and first cladding. Slight differences in doping concentrations allowed the multimode guiding part (i.e., within the first to second cladding) to feature the same numerical aperture (0.117) for all three fibers.

Fig. 3 shows the optical power at each output of the 3×1 MSPL for illumination in each input, at the end of the tapering process. The three curves represent the ratio of input power measured at the output when a single input is illuminated. The curve corresponding to the illuminated input remains close to 0 dB and represents insertion loss. The two other curves correspond to the fraction of input power transferred to each other output, i.e., crosstalk or inter-modal isolation. The MSPL characterized in Fig. 3 was realized with the DCFs described above, and using a synthetic fused silica capillary tube (CV1012, Vitrocom, NJ, USA). The length of DCF in a device can range from tens of centimeters to several meters. For the devices highlighted herein, during the fabrication process, we kept 1 m of DCF before the taper and 30 cm on the other end. We also spliced both ends of the DCFs to at least one meter of SMF-28 to ensure optimal single-mode performance. The losses at the splices between SMF-28 and DCF were negligible, i.e., comparable to splices between two SMF-28 fibers. Fig. 3(a) shows the power transfer for illumination into Input 1 consisting of the DCF with the largest inner cladding, expected to excite a supermode akin to the first linearly-polarized (LP) mode, LP_{01}, in the fused section. Results show power transfer with ≤ 1.84 dB excess loss into Output 1 (black curve), and ≥ 20 dB extinction in Output 2 (blue curve) and Output 3 (red curve) ports, respectively. Similarly, Fig. 3(b) shows the power transfer for illumination into Input 2, the DCF with the second largest inner cladding, expected to excite a supermode akin to LP_{11a} in the fused section. Results show quasi-lossless transfer (≤ 0.64 dB excess loss) into Output 2 (blue curve), and ≥ 20 dB extinction in Outputs 1 (black curve) and 3 (red curve), respectively. Finally, Fig. 3(c) shows the power transfer for illumination into Input 2, the DCF with the smallest inner cladding, expected to excite a supermode akin to LP_{11b} in the fused section. Results show power transfer with ≤ 1.65 dB excess loss into Output 3 (red curve), and ≥ 20 dB extinction in Outputs 1 (black curve) and 3 (red curve), respectively.
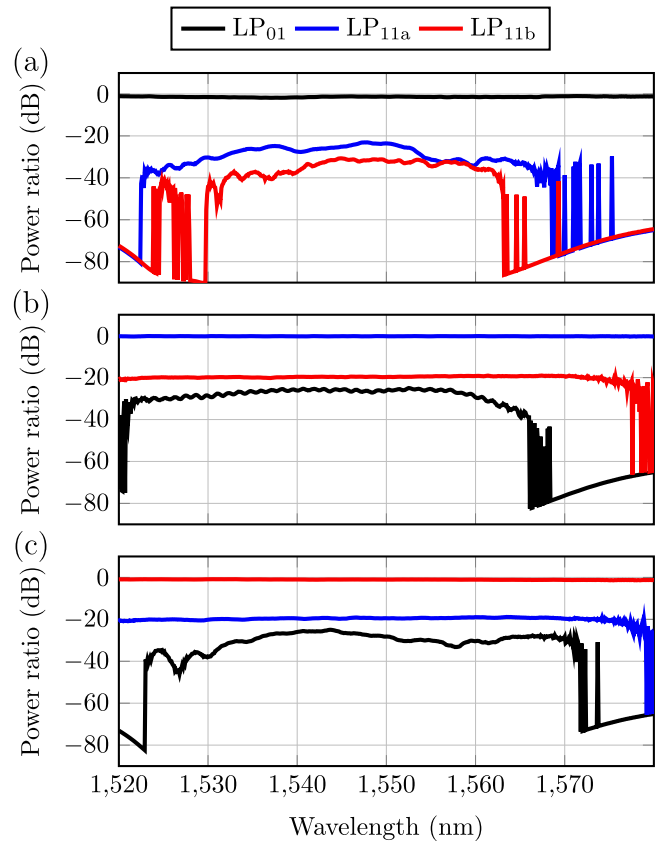

Fig. 3. Differential power measurements at the output of a 3×1 lantern inside a capillary tube made of synthetic fused silica with a slightly lower index of refraction than that of the outer cladding of the fibers. The measurement is made at the end of the fusion-taper process, before cleaving. (a): core illumination through the fiber with the largest first-cladding diameter, resulting in the fundamental mode, akin to LP_{01}, in the few-mode section. (b): core illumination through the fiber with the second largest first-cladding diameter, which generates the next mode, akin to LP_{11a}. (c): illumination through the fiber with the smallest first-cladding diameter, which generates the last guided mode, akin to LP_{11b}.

Fig. 4 shows the optical power at each output of the 3×1 MSPL for illumination in two different inputs, right at the end of the tapering step. For this MSPL, the three DCFs were arranged inside a fluorine-doped fused silica capillary tube (FTB03, Thorlabs, NJ, USA). Fig. 4(a) shows the power transfer for illumination into Input 1, the DCF with the largest inner cladding, expected to excite a supermode akin to LP_{01} in the fused section. Results show power transfer with ≤ 0.49 dB excess loss into Output 1 (black curve), and ≥ 60 dB extinction in Output 2 (blue
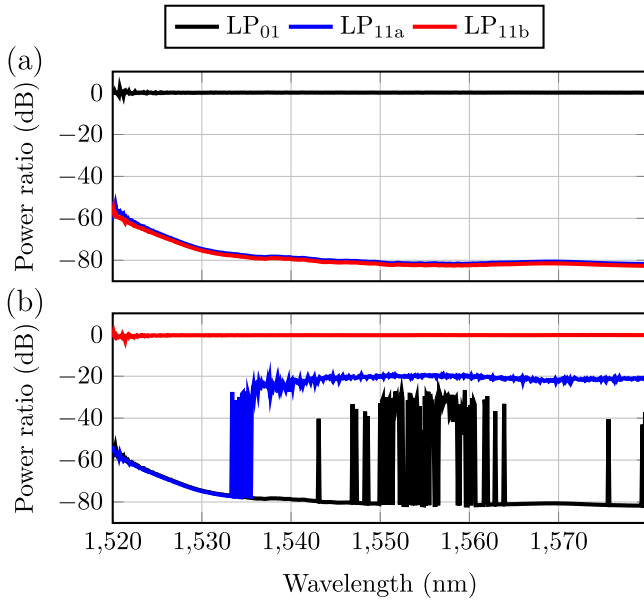
Fig. 4. Differential power measurements at the output of a 3×1 lantern inside a capillary tube made of fluorine-doped silica, with an even lower index of refraction than that of the outer cladding of the fibers. (a): core illumination through the fiber with the largest first-cladding diameter, resulting in the fundamental mode, akin to LP_{01}, in the few-mode section. ((b): illumination through the fiber with the smallest first-cladding diameter, which generates the last guided mode, akin to LP_{11b}. An accidental break of the third fiber resulted in it not being illuminated during that run.
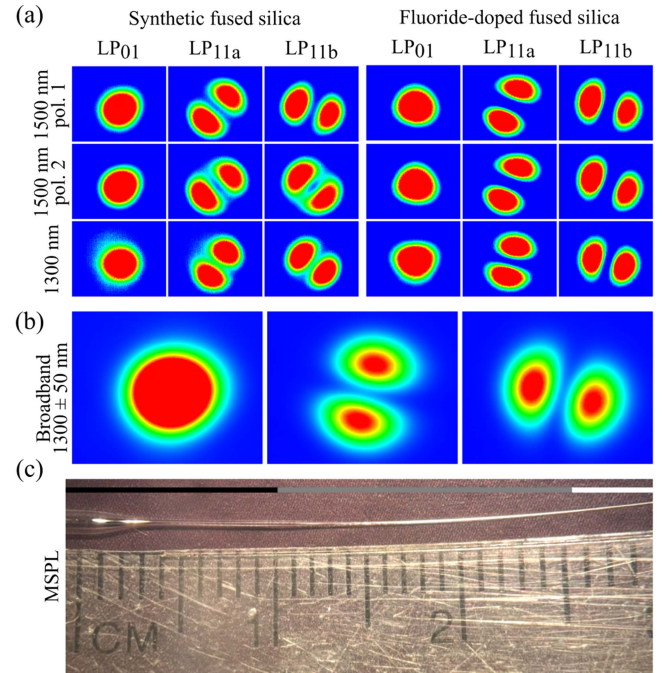

Fig. 5. Far-field images of the modes at the output of the few-mode section, illuminating through each of the single-mode fiber input to generate (a) LP_{01}, (b) LP_{11a}, and (c) LP_{11b}. (d) Picture of the photonic lantern under microscope.

curve) and Output 3 (red curve) ports, respectively. Similarly, Fig. 4(b) shows the power transfer for illumination into Input 3, the DCFs with the smallest inner cladding, expected to excite a supermode akin to LP_{11b} in the fused section. Results show quasi-lossless transfer (≤ 0.46 dB excess loss) into Output 2 (blue curve), and ≥ 20 dB extinction in Outputs 1 (black curve) and 3 (red curve), respectively. Power transfer for illumination into Input 2 was not recorded for this component. However, the coupling between the two branches is the same in both directions: illuminating Input X and measuring the loss in Output Y gives the same information as illuminating Input Y and measuring the loss in Output X. This can indeed be observed in Fig. 3, e.g. comparing the red trace in Fig. 3(b) to the blue trace in Fig. 3(c). In that respect, apparently anomalous points in the black curve of Fig. 4(b), which should follow the red curve of Fig. 4(a), and does so most of the time, are probably due to micro stresses (fibers moving) during the fast measurement. In the end, the only information missing from the lack of illumination in Input 2 is the excess loss for the corresponding fiber. It is, however, expected to be in line (≤ 0.5 dB) with that of the fibers corresponding to Inputs 1 and 3, as is usually the case.

After the fusion and tapering process, both structures were cleaved, and each input port was individually illuminated to capture an optical profile. A fiber polarization controller was used to characterize the component's behavior with respect to input polarization. An image in the far field was obtained by projecting each output onto a screen and recording using an infrared camera (SU320KTS-1.7RT, Goodrich, NJ, USA). Narrow-band illumination at 1300 nm and 1550 nm was achieved with a

dual-wavelength source (HP 8153ASM, Hewlett-Packard, CA, USA). A broad source (100 nm wide around 1300 nm) was used for broadband illumination (SL1310V1-10048, Thorlabs, NJ, USA).

Fig. 5(a) shows the optical profile in the far field of an MSPL based on a synthetic fused silica capillary (left) and based on a fluorine-doped fused silica capillary (right), respectively. For each group, the left column shows the fundamental mode of the structure (akin to LP_{01}) when the largest first-cladding diameter is illuminated. The center and right columns, respectively, show the two other modes (akin to LP_{11a} and LP_{11b}, respectively) in orthogonal orientations when the other two inputs are illuminated. The first two rows correspond to narrow-band illuminations at 1550 nm, with two different polarization states finding the most significant difference between each mode. They show that the behavior of the components is independent of the polarization state of the illumination source. The third row corresponds to narrow-band illumination at 1300 nm. and Fig. 5(b) shows the optical profile using broadband illumination around 1300 nm for LP_{01}, LP_{11a}, and LP_{11b}, respectively, for the fluorine-doped capillary tube MSPL. On the surface, the response at 1300 nm appears almost identical to that at 1550 nm. Although a good indication, this is not sufficient to claim that the component is broadband. Using broadband sources in the fabrication process and recording isolation and excess losses at all wavelengths will be necessary to characterize the operational bandwidth properly. Fig. 5(c) shows a section of the final structure of the MSPL, which is divided into three main parts. From left to right: With a black line above, a 1 cm taper of the capillary tube designed to constrain the DCFs. At this point, no tapering of the three-fiber bundle has taken place yet. With a grey line
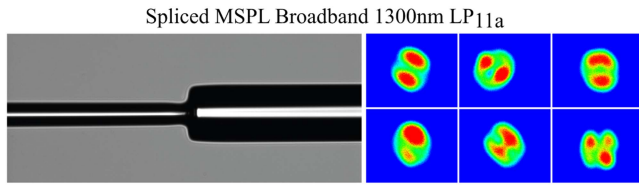
Spliced MSPL Broadband 1300nm LP$_{11a}$

Fig. 6. Few-mode section of MSPL spliced to a regular few-mode fiber. Left: picture of the splice in the Vytran GPX-30 splicer. Right: optical profiles at the output of the few-mode fiber after injecting light into the LP$_{11a}$ port of the lantern.

above, a 1.5 cm taper of the whole structure. And finally, with a white line above, a 0.3 cm section of the few-mode structure. This last section continues further outside of the image, but it is better to cleave it close to the grey-to-white transition, as the grey and white parts are the most fragile sections and should be kept below 2.5 cm to ensure sturdiness.

Fig. 6 (left) showcases a splice between the few-mode section of an MSPL and a two-mode step-index fiber (FM2010-B, YOFC, CN). On the right of Fig. 6, various intensity profiles have been captured when the lantern is illuminated in the LP$_{11a}$ input with a broadband source centered around 1300 nm. Since LP$_{11a}$ and LP$_{11b}$ are degenerate in the two-mode step-index fiber, they couple and rotate inside that section, and various optical profiles can be obtained by slightly perturbing (e.g., bending or heating) the fiber. In applications requiring mode isolation between the LP$_{11}$ modes, a modified few-mode fiber that is not degenerate for these modes should be spliced instead, or the photonic lantern should be coupled to free space without additional splice [20].

IV. DISCUSSION

The components fabricated for this study exhibited excess low loss: < 1 dB for the components held in a fluorine-doped capillary tube and < 2 dB for the component held in synthetic fused silica. They also feature large modal isolation above 20 dB, and in the case of the fluorine-doped components above 60 dB, the measurement being limited only by the noise floor of the measuring device.

For both components characterized in Figs. 3 and 4, the operational bandwidth was limited by the bandwidth of the illumination laser (JDS Uniphase 1550 nm). As such components do not rely on mode coupling, they are theoretically as broadband as the guiding properties of the fibers allow.

As shown [24], SuPyMode offers significant insight into the fabrication processes for various optical fiber devices, including MSPLs. It achieves this through the computation of the adiabatic criterion, which dictates the steepest adiabatic taper slope and is thus directly related to the minimum length of the device [24]. Some simulations show that the use of DCFs can offer a decrease in the total length by a factor of 3 compared to standard MSPLs (see Supplementary Material).

A comparison of the results between the two components shows that using a higher index difference between the outer cladding of the fibers and the external capillary tube usually leads to better modal isolation and lower excess losses. Although the fluorine-doped capillary tubes give overall better results, they are much more expensive than those made of synthetic

fused silica. In principle, the fabrication process enables two lanterns to be extracted from each fused and tapered bundle, by cleaving exactly in the middle of the tapered section. However, the component is not fully symmetric to start with. Fiber insertion within the capillary tube requires stripping the coating over a distance of at least 20 cm longer than the capillary, on one of its sides. For two lanterns to be made out of the component, re-coating of that section is required to avoid fragility.

In theory, the fabrication of MSPLs should never result in fiber-to-fiber coupling, in contrast to what is expected for couplers. Any such power transfer is thus indicative of a flaw in the device or a non-adiabatic section caused by too steep a transition (e.g., a micro bend) in the device. Real-time monitoring enables these types of flaws to be immediately detected. In-situ monitoring also enables the measurement of actual mode isolation and excess loss, contrary to the cutback method, which measures losses from each input into the few-mode section after cleaving. This method widely underestimates excess losses as it does not measure cladding or coupling losses. For instance, for the component made with a synthetic silica tube, we measured excess losses of 1.84, 0.64, and 1.65 dB for Inputs 1,2 and 3, respectively. But the cutback technique, performed after cleaving, gave 0.08, 0.10, and 0.11 dB for the same Inputs, respectively. Note that we did not remove cladding material for the cut-back technique. This could result in underestimating losses as some cladding light could be counted as transmitted. In all cases, we believe the in-situ technique provides a better measurement of losses.

Double-clad fiber-based MSPLs allow for high modal isolation; however, the resulting modes are not quite perfectly matched to the theoretical LP modes. Some mode asymmetry was observed, likely due to the final shape of the few-mode section, which is not perfectly cylindrical.

Lastly, scalability of MSPLs is achieved by varying the characteristics of each individual fiber in the bundle. With single-clad fibers, or indeed with DCFs, this can be achieved by changing the diameter of the core. It has, for instance, been demonstrated that a change in diameter of 3 μm achieves significant mode selectivity [14]. Unfortunately, it comes at the cost of single-mode compatibility. Graded-index fibers can also be used, and their designs vary to achieve some degree of scalability, but again at the cost of single-mode compatibility. DCFs offer another possibility, which is to vary the outer diameter of the first cladding. This can be achieved while maintaining single-mode compatibility. As the first cladding effectively becomes a new core in the tapered structure, and as coupling between modes essentially depends on the distance between cores [13], we expect that changes of 3 μm will be sufficient to introduce selectivity. To maintain single-mode operation, the first cladding outer diameter must fall between 15 and 70 μm. This allows for potentially up to 18 separate modes to be multiplexed. Should more modes be required, additional cladding layers could be added, although systematic research has to be undertaken to verify this. Currently, the main advantage of using DCFs is that they allow for at least equivalent scalability compared to other types of fibers, with the added bonus of single-mode compatibility.

V. Conclusion

The use of DCFs in the design of MSPLs provides a versatile means to break symmetries by varying the first-cladding diameter while retaining full compatibility with single-mode fibers. This allows for complete characterization of the devices in real-time during fabrication.

The adiabatic criteria of the DCF-based components is slightly lower than those made of graded-index fibers. However, they are high enough that short ($\simeq 2.5$ cm), sturdy components can be fabricated with relative ease. Our experiments confirm that MSPLs in general keep their characteristics over large bandwidths (at least 250 nm in this study) and are agnostic to the state of polarization of the illumination.

Components held in synthetic fused silica capillary tube have higher overall excess losses and lower modal isolation figures than those held in fluorine-doped capillary tubes. However, the former are much cheaper than the latter, and they provide a good alternative for components that do not require the best specifications.

Disclosures

Acknowledgment

References

[1] S. G. Leon-Saval, T. A. Birks, J. Bland-Hawthorn, and M. Englund, "Multimode fiber devices with single-mode performance," *Opt. Lett.*, vol. 30, pp. 2545–2547, Oct. 2005.

[2] N. K. Fontaine et al., "Photonic lanterns, 3-D waveguides, multiplane light conversion, and other components that enable space-division multiplexing," *Proc. IEEE*, vol. 110, no. 11, pp. 1821–1834, Nov. 2022.

[3] J. Fang et al., "Performance optimization of multi-plane light conversion (mplc) mode multiplexer by error tolerance analysis," *Opt. Exp.*, vol. 29, no. 23, pp. 37852–37861, Nov. 2021.

[4] N. K. Fontaine et al., "Broadband 15-mode multiplexers based on multiplane light conversion with 8 planes in unwrapped phase space," in *Proc. 2022 Eur. Conf. Opt. Commun.*, 2022, pp. 1–4.

[5] M. Hout et al., "Transmission of 273.6 tb/s over 1001 km of 15-mode multi-mode fiber using c-band only 16-qam signals," *J. Lightw. Technol.*, vol. 42, no. 3, pp. 1136–1142, Feb. 2024.

[6] S. Bade et al., "Fabrication and characterization of a mode-selective 45-mode spatial multiplexer based on multi-plane light conversion," in *Proc. 2018 Opt. Fiber Commun. Conf. Expo.*, 2018, pp. 1–3.

[7] N. K. Fontaine et al., "Hermite-Gaussian mode multiplexer supporting 1035 modes," in *Proc. 2021 Opt. Fiber Commun. Conf. Exhib.*, 2021, pp. 1–3.

[8] G. Labroille et al., "Characterization and applications of spatial mode multiplexers based on multi-plane light conversion," *Opt. Fiber Technol.*, vol. 35, pp. 93–99, 2017.

[9] J. D. Love and N. Riesen, "Mode-selective couplers for few-mode optical fiber networks," *Opt. Lett.*, vol. 37, no. 19, pp. 3990–3992, Oct. 2012.

[10] H. Guo, Y.-G. Liu, L. Chen, X. Wang, Z. Zhang, and Z. Wang, "Wavelength insensitive mode selective coupler based on ultra-wideband resonant effect," *J. Lightw. Technol.*, vol. 42, no. 17, pp. 6042–6048, Sep. 2024.

[11] H. Guo et al., "Ultra-low-loss 5-LP mode selective coupler based on fused biconical taper technique," *Opt. Exp.*, vol. 31, pp. 18050–18062, May 2023.

[12] S. H. Chang et al., "All-fiber 6-mode multiplexers based on fiber mode selective couplers," *Opt. Exp.*, vol. 25, no. 5, pp. 5734–5741, Mar. 2017.

[13] T. A. Birks, I. Gris-Sánchez, S. Yerolatsitis, S. G. Leon-Saval, and R. R. Thomson, "The photonic lantern," *Adv. Opt. Photon.*, vol. 7, pp. 107–167, Jun. 2015.

[14] A. M. Velázquez-Benítez et al., "Scaling photonic lanterns for space-division multiplexing," *Sci. Rep.*, vol. 8, no. 1, 2018, Art. no. 8897.

[15] J.-C. Olaya, S. G. Leon-Saval, D. Schirdewahn, K. Ehrlich, D. M. Haynes, and R. Haynes, "1:61 photonic lanterns for astrophotometry: A performance study," *Monthly Notices Roy. Astron. Soc.*, vol. 427, pp. 1194–1208, Dec. 2012.

[16] S. G. Leon-Saval, A. Argyros, and J. Bland-Hawthorn, "Photonic lanterns," *Nanophotonics*, vol. 2, pp. 429–440, Dec. 2013.

[17] C. H. Betters, S. G. Leon-Saval, J. G. Robertson, and J. Bland-Hawthorn, "Beating the classical limit: A diffraction-limited spectrograph for an arbitrary input beam," *Opt. Exp.*, vol. 21, pp. 26103–26112, Nov. 2013.

[18] I. Ozdur, P. Toliver, A. Agarwal, and T. K. Woodward, "Free-space to single-mode collection efficiency enhancement using photonic lanterns," *Opt. Lett.*, vol. 38, pp. 3554–3557, Sep. 2013.

[19] A. M. Velázquez-Benítez, K. Y. Guerra-Santillán, R. Caudillo-Viurquez, J. E. Antonio-López, R. Amezcua-Correa, and J. Hernández-Cordero, "Optical trapping and micromanipulation with a photonic lantern-mode multiplexer," *Opt. Lett.*, vol. 43, pp. 1303–1306, Mar. 2018.

[20] M. P. de Sivry-Houle, S. B. Beaudoin, S. Brais-Brunet, M. Dehaes, N. Godbout, and C. Boudoux, "All-fiber few-mode optical coherence tomography using a modally-specific photonic lantern," *Biomed. Opt. Exp.*, vol. 12, pp. 5704–5719, Sep. 2021.

[21] R. Maltais-Tariant, R. I. Becerra-Deana, S. Brais-Brunet, M. Dehaes, and C. Boudoux, "Speckle contrast reduction through the use of a modally-specific photonic lantern for optical coherence tomography," *Biomed. Opt. Exp.*, vol. 14, pp. 6250–6259, Dec. 2023.

[22] R. Maltais-Tariant, M. Dehaes, and C. Boudoux, "Exact measurement of transverse flow velocity using few-mode optical coherence tomography," *Proc. SPIE*, vol. PC12367, 2023, Art. no. PC123670G.

[23] L. Shen et al., "Highly mode selective 3-mode photonic lantern through geometric optimization," presented at Opt. Fiber Commun. Conf., San Diego, CA, USA, Mar. 11–15, 2018, Paper W2A.14.

[24] M. Poinsinet de Sivry-Houle, R. I. Becerra-Deana, S. Virally, N. Godbout, and C. Boudoux, "Supymode: An open-source library for design and optimization of fiber optic components," *Opt. Continuum*, vol. 3, no. 2, pp. 242–255, Feb. 2024.

[25] S. Sunder and A. Sharma, "Engineering adiabaticity for efficient design of photonic lanterns," *IEEE Photon. J.*, vol. 13, no. 2, Apr. 2021, Art. no. 2200113.

[26] B. Huang et al., "All-fiber mode-group-selective photonic lantern using graded-index multimode fibers," *Opt. Exp.*, vol. 23, pp. 224–234, Jan. 2015.

[27] K. Harrington, S. Yerolatsitis, D. V. Ras, D. M. Haynes, and T. A. Birks, "Endlessly adiabatic fiber with a logarithmic refractive index distribution," *Optica*, vol. 4, pp. 1526–1533, Dec. 2017.

[28] D. Donlagi and B. Culshaw, "Propagation of the fundamental mode in curved graded index multimode fiber and its application in sensor systems," *J. Lightw. Technol.*, vol. 18, no. 3, pp. 334–342, Mar. 2000.

[29] P. Chanclou et al., "Expanded single-mode fiber using graded index multimode fiber," *Opt. Eng.*, vol. 43, no. 7, pp. 1634–1642, 2004.

[30] Y. Mizuno and K. Nakamura, "Core alignment of butt coupling between single-mode and multimode optical fibers by monitoring brillouin scattering signal," *J. Lightw. Technol.*, vol. 29, no. 17, pp. 2616–2620, Sep. 2011.

[31] M. J. Adams, D. N. Payne, and F. M. E. Sladen, "Splicing tolerances in graded-index fibers," *Appl. Phys. Lett.*, vol. 28, pp. 524–526, Aug. 2008.

[32] N. K. Fontaine, R. Ryf, J. Bland-Hawthorn, and S. G. Leon-Saval, "Geometric requirements for photonic lanterns in space division multiplexing," *Opt. Exp.*, vol. 20, pp. 27123–27132, Nov. 2012.

[33] S. A. Tedder et al., "Single-mode fiber and few-mode fiber photonic lanterns performance evaluated for use in a scalable real-time photon counting ground receiver," *Proc. SPIE*, vol. 10910, pp. 69–78, Mar. 2019.

[34] J. J. Davenport, M. Diab, K. Madhav, and M. M. Roth, "Optimal SMF packing in photonic lanterns: Comparing theoretical topology to practical packing arrangements," *J. Opt. Sociaty Amer. B*, vol. 38, pp. A7–A14, Jul. 2021.

[35] R. I. Becerra-Deana, M. P. de Sivry-Houle, S. Bolduc-Beaudoin, C. Boudoux, S. Virally, and N. Godbout, "Short mode-selective photonic lanterns using double-clad fibers," *Proc. SPIE*, vol. PC12428, 2023, Art. no. PC1242802.

[36] C. Zhang, Y. Wang, S. Zhang, M. Xiang, S. Fu, and Y. Qin, "Low-loss and compact photonic lantern based on a step-index double cladding fiber," *Opt. Lett.*, vol. 49, no. 9, pp. 2277–2280, May 2024.

Rodrigo Itzamná Becerra-Deana is currently working toward the Ph.D. degree with the Fiber Optics Laboratory and the Laboratory for Optical Diagnoses and Imaging, Engineering Physics Department, Polytechnique Montréal, Montreal, QC, Canada. He is also with Castor Optics, where he develops novel fiber components.

Martin Poinsinet de Sivry-Houle is currently a Research Fellow with the Engineering Physics Department, Polytechnique Montréal, Montreal, QC, Canada. He developed SuPyMode, the library used in all the simulations for the design of fiber components in the Fiber Optics Laboratory.

Stéphane Virally (Member, IEEE) is currently a Research Fellow with the Engineering Physics Department, Polytechnique Montréal, Montreal, QC, Canada. He is a Co-Inventor of more than 15 patents worldwide. He also leads the Fiber Optics Laboratory.

Caroline Boudoux is currently a Professor of engineering physics with Polytechnique Montréal, Montreal, QC, Canada. She founded the Laboratory for Optical Diagnoses and Imaging and co-founded Castor Optics, inc. She has authored or coauthored numerous publications, patents, and books on topics ranging from biomedical optics to engineering design, and doctoral studies. She is SPIE Fellow, and Director-at-Large with Optica.

Nicolas Godbout is currently a Professor and the Director of the Engineering Physics Department, Polytechnique Montréal, Montreal, QC, Canada. He was with the Fiber Optics Laboratory for more than 15 years and has 25 years of experience in the design and fabrication of fiber components for applications in telecommunications, biophotonics and quantum optics. He is a Co-Inventor of more than ten patent families that are actively exploited. He is also a Co-Founder of Castor Optics which develops and manufactures novel optical fiber components for various markets.